Thermochemical aspects of boron and phosphorus distribution between silicon and $BaO\text{-}SiO_2$ and $CaO\text{-}BaO\text{-}SiO_2$ slags

Jafar Safarian*

* Norwegian University of Science and Technology (NTNU), Alfred Getz Vei 2, No-7491, Trondheim, Norway, Jafar.Safarian@ntnu.no

Abstract

In the production of solar grade silicon by metallurgical route the distribution of B and P between slags and liquid silicon is the most important key issue. The equilibrium and thermochemistry of reactions between liquid silicon and $BaO\text{-}SiO_2$ slags and up to 10% BaO-containing $CaO\text{-}BaO\text{-}SiO_2$ slags is studied through experimental work and using thermodynamic calculations. It is shown that the distribution coefficient of B (L_B) is higher for the $CaO\text{-}BaO\text{-}SiO_2$ slags than that for $BaO\text{-}SiO_2$ slags and it is not significantly affected by temperature and composition changes of the slags. In contrast, the distribution coefficient of P (L_P) is higher for $BaO\text{-}SiO_2$ slags than that for the $CaO\text{-}BaO\text{-}SiO_2$ slags, and it is higher at lower temperatures. The chemical activities of the dilute solutions of Ba in liquid silicon, and the dilute solutions of B_2O_3, P_2O_5 and BaO in the slags are calculated. Moreover, the reaction mechanisms for B, P, Ba and Ca transport between liquid silicon and the slags are explained.

Key words: Silicon, Boron, Phosphorous, barium, calcium, slag, distribution coefficient

1. Introduction

Silicon is liberated from its natural oxide form (quartz) through a carbothermic reduction process in submerged electric arc furnace; the product being metallurgical grade silicon (MG-Si), which is further purified to reach solar grade silicon (SoG-Si) quality for PV applications. The purity of MG-Si isusually above 99% Si and it contains impurities such as Fe, Al, Ti, Ca, B, and P [1], while SoG-Si has much higher purity of above 99.9999 %Si. The majority of SoG-Si feedstock in the market is currently produced from MG-Si through the well known *Siemens process* or newly developed *fluid bed reactor (FBR)* technology. In these chemical processes, pure silicon is deposited on rods or silicon seeds from a gas phase, which is produced through the conversion of MG-Si to purified gaseous compounds of silicon; $SiHCl_3$ or SiH_4. The Siemens process in particular is an expensive process with regard to high energy consumption [2, 3]. However, the production of SoG-Si through *metallurgical refining processes* is more energy efficient and environmentally friendly than chemical route which in turn may encourage a faster growth of the global PV market. This has been the motivation for the development of several refining processes, where MG-Si is refined through the combination of sub-processes to produce SoG-Si. Almost all the present impurities in MG-Si except B and P can be effectively removed by directional solidification, which is a final key process step in metallurgical approaches. Boron is the most difficult element to be removed by directional solidification due to its large distribution coefficient between solid and liquid phases, which is $K_B=0.8$ [4]. In order to remove this impurity, many potential processes have been studied such as slag refining, plasma refining, gas refining, solvent refining, leaching, etc. [3]. In particular, the slag refining technique is a part of the only commercial metallurgical process of *ELKEM Solar* for SoG-Si production, where the dissolved B in silicon is adsorbed to a silicate slag through oxidation. Hence, the potential of slags for B removal is the main important parameter to consider for the process. In this case, the thermodynamic equilibrium for B distribution

between liquid silicon and molten slags is studied, which is defined based on the weight percentages of B in the two phases as:

$$L_B = \frac{(wt\%B)_{slag}}{[wt\%B]_{metal}} \quad (1)$$

The magnitude of L_B-*value* is depending on slag type and composition, temperature, gas phase composition and as it is a quite important parameter it has been extensively studied through many experimental works for many silicate slag systems. For instance, many slags such as $CaO\text{-}SiO_2$ [5, 6, 7, 8, 9, 10], $CaO\text{-}CaF_2\text{-}SiO_2$ [6, 8, 11,12], $CaO\text{-}BaO\text{-}SiO_2$ [6], $CaO\text{-}MgO\text{-}SiO_2$ [5, 6, 13], $CaO\text{-}Al_2O_3\text{--}SiO_2$ [14], $CaO\text{-}Na_2O\text{-}SiO_2$ [14, 15], $Al_2O_3\text{-}CaO\text{-}MgO\text{-}SiO_2$ [16], $Al_2O_3\text{-}BaO\text{-}SiO_2$ [16] and $Al_2O_3\text{-}CaO\text{-}MgO\text{-}SiO_2$ [16] , $Na_2O\text{-}SiO_2$[17] and $CaO\text{-}Na_2O\text{-}SiO_2$ slags[18] have been studied experimentally. In general L_B is increased with increasing temperature as been observed through the studies using $CaO\text{-}SiO_2$ slags [6], $CaO\text{-}CaF_2\text{-}SiO_2$ slags [6, 12], and $CaO\text{-}Na_2O\text{-}SiO_2$ slags [14, 15]. The relationship between L_B and slag chemical composition is complicated and L_B in a wide range from 0.3 for $CaO\text{-}SiO_2$ slags to 9.3 [6] for $CaO\text{-}Al_2O_3\text{-}SiO_2$ slags [14] have been reported by different researchers. Inspecting the literature data it is seen that the measured L_B values for a given slag system are not in agreement. For instance, the reported L_B values by Teixeira et al. [8] using $CaO\text{-}SiO_2$ slags are in the range of 2 to 5.5, L_B is in the minimum at CaO/SiO_2=0.85 and it is increased with both decreases and increases of the slag basicity. However, much narrower L_B range for the same slag system has been observed in which L_B is not significantly affected by the slag chemical composition and it is increaseed minimally from 2.2 to 2.5 with increasing the basicity from 0.6 to 1.3 [9]. It has to be noticed that the analysis of B in low concentrations in both Si and slag phases is a challenge and this issue may be a reason for observing different results in similar

experiments, in addition to other sources of errors. The recent studies on using Na_2O-SiO_2 [17] and CaO-Na_2O-SiO_2 [18] slags have shown that when Na_2O-containog slags are contacted with silicon the dissolved B is also gasified in the form of sodium metaborate ($Na_2B_2O_4$) due to its relative high vapor pressure in the system as its mechanism has been explained. [17, 18]

In the present study the distribution of B and also P between silicon and BaO-SiO_2 and CaO-BaO-SiO_2 slags is studied. In addition to B distribution, the P distribution between slags and silicon is studied as it is more concentrated in the silicon phase and it may affect further silicon purification processes, i. e. acid leaching. The involved reactions for the mass transport of Ba, Ca, B and P between the silicon and slag phases are studied. The thermodynamic activities of the solute elements in the silicon and slag phases are determined through applying the fundamental thermochemical approaches, employing thermodynamic tables and software.

2. Experimental procedure

In the present study, specific silicon and slag samples were produced and further interacted at elevated temperatures through the following described methodology.

2.1. Materials preparation

Two types of BaO-containing slags were prepared by mixing high purity powders of BaO, CaO and SiO_2 powders (+99%) and melting the mixtures in high purity graphite crucibles. The slags were BaO-SiO_2 binary slags, and BaO-CaO-SiO_2 slags containing up to 10%BaO, the initial compositions for these slags are given in Table 1. All the target slag compositions are in molten state at the target reaction temperatures, according to the related binary and ternary slag systems. The slags were prepared through heating up the mixtures to 1923±30 K (1650±30˚C)

and holding for around one hour for complete melting, followed by slow cooling to the room temperature.

High purity electronic grade silicon was doped by B and P elements through mixing with two high purity Si-B and Si-P master alloys, which were containing 500 ppm B and 1300 ppm P, respectively. The applied procedures for making these two master alloys were described previously [19, 20]. The silicon mixtures were melted through their heating up to 1823 K (1550˚C) in a high purity graphite crucible in an induction furnace, holding at this temperature for 30 minutes and casting the melt in a water-cooled copper mold to attain a homogeneous silicon regarding the B and P concentrations. As a result, a silicon containing 30±1 ppmw B and 25±0.5 ppmw P was produced as analyzed by a high resolution Inductively Coupled Plasma-Mass Spectrometer (ICP-MS) on four samples. It is worth mentioning that the contamination of silicon by carbon is not significant as the solubility of carbon in silicon is low, i.e. 150 ppm at 1550 ˚C. This small amount of carbon have no significant effect on the chemical properties of B and P components, which is more acceptable when the concentrations are very low as this study.

2.2. Silicon and slag interaction

The B- and P-doped silicon sample was added into the slag-containing crucibles, while the slag/silicon mass ratio was fixed equal to 2. Then the crucibles were heated to 1773 K (1500˚C) and 1873 K (1600˚C) in an induction furnace under high purity Ar (99.999%Ar) flow. The samples were hold at the target temperatures for 2 hours, followed by slow cooling to the room temperature. As the electromagnetic forces extensively stir the molten silicon, it causes high mixing of the system and equilibrium is reached in the experiments duration. The solidified samples were then crushed and silicon and slag particles were separated. It is worth mentioning

that the solidified silicon and slag phases showed similar configuration in all crucibles (silicon melt is surrounded by slag phase) as observed previously in using Na_2O-SiO_2 slag [17] indicating complete melting and proper contact of the two phase. The samples were then analyzed for measuring the main components by ICP-MS. In this case, three parallels of each sample were analyzed and then the average compositions were determined.

3. Results

The results of the experiments are described as follows.

3.1. Mass transport between the phases and Ba and Ca distribution

The measured chemical compositions of the slags after interaction with silicon are given in Table 1. The chemical composition changes in this table show that there is significant mass transport between the two phases so that the concentrations of Ba, Ca and Si in the slags are significantly different compare to the initial slag concentrations. However, no significant changes in the main slag components is observed for the experiments 8, 9 and 12. This may indicate that the slags 8 and 9 are in almost equilibrium with molten silicon. However, experiment 10 result may indicate that BaO in low concentrations has a high affinity into the CaO-SiO_2 slags (with CaO/SiO_2 =0.67) and it is not reduced at 1500˚C when up to 2.5 %BaO exists in the slag. The measured concentrations of Ba in silicon interacted with the binary BaO-SiO_2 slags (Fig.1) show that the solubility of Ba in silicon is increased with increasing the slag basicity (BaO/SiO_2 ratio), indicating there is larger driving force for the mass transport of Ba from the barium-silicate slags into the liquid metal for higher basicities. Moreover, the amount

of Ba in silicon is depending on the process temperature. Fig. 1 shows that more Ba is transferred from the slags into silicon at the higher temperature, while there is slightly different trends at the two temperatures for Ba concentration dependence on basicity changes.

The measured concentrations for experiments 9 to 14 show that the mass transport of both Ca and Ba from the slag into the silicon occurs; Ca for CaO-SiO_2 slags and the both elements in CaO-BaO-SiO_2 slags. Fig. 2 shows that Ba transfer into liquid silicon is increased with increasing the concentration of BaO in the initial slag for a given temperature and initial CaO/SiO_2 ratios. Regarding the concentrations in Table 1, there is significant reduction in basicity ((wt%CaO+wt%BaO)/wt%SiO_2) when BaO exists in the slag, and considerable reductions of BaO and CaO occurs, which is accompanied with Si transfer as SiO_2 into the slag. According to Table 1 and Figs. 1 and 2, the transfer of Ba and Ca into liquid silicon for a given initial chemical composition is significantly higher at 1873 K (1600˚C) than 1773 K (1500˚C). Figure 3 shows the relationship between X_{Ba}/X_{Ca} molar ratio and X_{BaO}/X_{CaO} molar ratio in metal and slag phases, respectively. A direct relationship between these concentration ratios in the two phases is observed and larger X_{Ba}/X_{Ca} ratio for higher BaO concentrations in the initial ternary slags. However, it is observed that for a given BaO/CaO ratio there is higher Ba/Ca ratio in the metal phase at the lower temperature, evident of CaO reduction at 1873 K (1600˚C) is significantly more than that at 1773 K (1500˚C). It is worth noting that Ca and Ba transferred into the silicon are easily removed by directional solidification in the integrated solar silicon process.

3.2. The distribution of phosphorus

The distribution coefficient of P between the slag and silicon phases (L_P) can be calculated based on the measured P concentrations in the two phases using the following expression:

$$L_P = \frac{(wt\%P)_{slag}}{[wt\%P]_{metal}} \quad (2)$$

Figure 4 shows the relationship between L_P and basicity for the binary BaO-SiO_2 slags in contact with silicon. Obviously, the L_P value is depending on temperature and it is larger for lower temperatures. Moreover, L_P is not significantly depending on the basicity, and it is increased or decreased minimally with basicity changes, however, different trends for the two temperatures are observed. The distribution of P between CaO-(BaO)-SiO_2 slags and silicon in Fig. 5 indicates that there is again larger L_P values for the lower temperature for a given slag basicity. Moreover, the L_P value is increased at 1773 K (1500˚C) with increasing the basicity, or in another word the introduction of BaO-containing slags possess high phosphate capacity. However, the L_P change with basicity change is not significant at 1873 K (1600˚C). This may show that the introduction of small amount of BaO into CaO-SiO_2 slag is beneficial for P removal. However, the both diagrams in Figs. 6 and 7 indicate that the effect of temperature on P distribution is the main parameter. It is worth mentioning that L_P for 20%Al_2O_3-BaO-SiO_2 slags for BaO/SiO_2 between 0.45 to 1.3 was studied by Johnston and Barati [16] and the measured L_P between 0.1 to 0.2 at 1773 K (1500˚C), which is lower than the L_P in this study.

3.3. The distribution of boron

The measured concentrations of B between the slag and metal phases were used to calculate the distribution coefficient of B between the two phases by Eq. (1) and the results for the BaO-SiO_2 slags and CaO-BaO-SiO_2 slags are shown in Figs. 6 and 7, respectively. These figures

show that L_B is significantly lower for BaO-SiO_2 slags than that for low BaO-containing CaO-SiO_2 slags. L_B is in the range of 0.85 to 1.35 for BaO-SiO_2 slags, while for the other slag is in the range of 2.0 to 2.4. On the other hand, the relationship between the L_B and basicity in these slags is different. It is worth mentioning that Suzuki et al. [6] measured lower L_B-*values* for using CaO-10%BaO-SiO_2 slags at 1723K (1450˚C) and the obtained L_B between 1.45 to 1.9 for (CaO+BaO)/SiO_2 ratios between 0.8 to1.3, which are higher basicity range than the present study. As seen in Fig. 6, when the binary BaO-SiO_2 slag is contacted with liquid silicon, the L_B value is showing smaller value when the basicity is close to unity. However, for other studied basicities, up to around 30% higher L_B-value is observed. Moreover, L_B-value is higher for higher temperature for a given slag composition, meaning that more B is possible to be removed from silicon at higher temperatures, this may be the reason of obtaining higher L_B-values in this study than Suzuki et al. [6]. The changes of L_B with basicity for the CaO-(BaO)-SiO_2 slags in Fig. 7 show that L_B is not significantly affected by the introduction of small amount of BaO into the CaO-SiO_2 slag. Moreover, it is difficult to see a clear effect of temperature and L_B-*value* in a short range of 2.1±0.1 at 1600˚C, and 2.2±0.2 at 1500˚C. This insignificant temperature dependence of L_B is in agreement with literature for CaO-SiO_2 slag systems [27]. In contrast to L_P parameter, L_B is more dependent on the slag composition and less on process temperature.

4. Discussion

The obtained results presented in the previous section are discussed and they are used to determine some thermodynamics parameters in the studied slag-metal systems.

4.1. Mass transport of Ba into silicon and its chemical activity

When the binary $BaO\text{-}SiO_2$ slag reacts with the high purity liquid silicon, a portion of Ba is transferred into the molten silicon through the following reaction:

$$Si + 2(BaO) = 2\,\underline{Ba} + (SiO_2) \qquad K_3\ (at\ 1773\ K) = 1.05\times10^{-5} \qquad (3)$$

In addition, when a $BaO\text{-}CaO\text{-}SiO_2$ ternary slag is contacted with silicon, chemical reaction (4) takes place simultaneously in the system, yielding some dissolved Ca in the silicon melt:

$$Si + 2(CaO) = 2\,\underline{Ca} + (SiO_2) \qquad K_4\ (at\ 1773\ K) = 2.4\times10^{-9} \qquad (4)$$

The measured slag concentrationsat two different temperatures show that reaction (3) proceeds more at higher temperatures as observed in Figs. 1 and 2 for the two types of slags. The standard Gibbs energy of formation for reactions (3) and (4) are both positive, i.e. 168.7 kJ/mol and 289.5 kJ/mol at 1500˚C and 1600˚C, respectively. Therefore, we may conclude that the reason for the mass transport of Ba and Ca through chemical reactions (3) and (4) is the large negative standard deviation of silicon rich Si-Ba and Si-Ca melts from the ideal solution, or in other word a driving force existence for the reactions. The previously determined activity coefficient for the dilute solutions of Ca in silicon as 0.0032 [21] at the silicon melting point at 1687 K (1414˚C) supports this explanation. In order to calculate the thermodynamic activity of Ba in liquid silicon the results of experiments 1 to 8 can be used. Considering the changes in Gibbs energy of reaction (3) at equilibrium, ΔG_3°, we may express the chemical activity of the dissolved Ba in Si as:

$$a_{Ba} = \left[\frac{a_{Si}{a_{BaO}}^2}{a_{SiO2}} exp\left(\frac{-\Delta G_3^{\circ}}{RT}\right)\right]^{\frac{1}{2}} \qquad (5)$$

In this study a_i denotes the activity of component i in solution, R is the universal gas constant and T is absolute temperature. Regarding the low measured equilibrium concentrations of Ba in silicon, we have a dilute solution of Ba in Si and it is a fair approximation to assume ideal

behavior for silicon solvent; a_{Si} equal to unity. The chemical activities in BaO-SiO_2 solutions has been studied in literature through experimental and theoretical works [22,23,24,25]. Based on the measured activities for BaO and SiO_2 by Tyurnina et al. [23,24] at 1910 K (1637˚C), the chemical activities of these slag components were calculated by a regular solution approximation at 1773 K (1500˚C) and 1873 K (1600˚C). The calculated a_{BaO} and a_{SiO2} curves and their comparison with the reported data by Tyurnina et al. are illustrated in Fig. 8. Negative deviation from the ideal solution is clearly observed for the both slag components in a large composition range, in particular for the chemical composition ranges of the slags in Table 1.

The chemical activity of the dissolved Ba in silicon in contact with the BaO-SiO_2 slags can be calculated using the determined activities for BaO and SiO_2 components in Eq. (5) as the results are illustrated in Fig. 9. Considering the low concentrations of Ba in liquid silicon, the activity coefficient of Ba in dilute solutions can be calculated as $\gamma_{Ba}^{\circ} = 8.8 \times 10^{-5}$ and $\gamma_{Ba}^{\circ} = 12.5 \times 10^{-5}$ at 1773 K (1500˚C9 and 1873 K (1600˚C), respectively. These in turn yield a temperature relationship between the activities coefficients of Ba in Si-Ba dilute solutions as:

$$\gamma_{Ba}^{\circ} = 7.81 \times 10^{-4} - \frac{1.229}{T} \qquad (6)$$

As observed above, there is a large negative deviation from ideal solution for the silicon-rich Si-Ba solutions and due to the low chemical activity of Ba, the chemical reaction (3) proceeds when the BaO-SiO_2 slags are contacted with silicon, which causes significant Ba transport into the liquid silicon as shown in Fig. 1. The more Ba transport from the slag into silicon at higher temperatures for a given slag composition is mainly attributed to the higher activity of BaO in

the slags at higher temperatures, while the other chemical activities in chemical reaction (3) are less temperature dependent. In other word, there is a larger driving force for the chemical reaction (3) at higher temperatures. However, not significant BaO transport to silicon when the concentration of BaO is low in CaO-BaO-SiO_2 is due to the low chemical activity of BaO in the slag, which causes small Ba transfer into Si (Fig. 2). Obviously, equilibrium is established by small BaO concentration in the slag, i.e. 2.5wt%BaO, while it occurs with more Ba transfer at higher concentrations and temperatures.

4.2. Chemical activity of BaO in low BaO-containing CaO-SiO_2 slags

The mass transport of Ba through chemical reactions (3) occurs rapidly through the contact of slag and liquid silicon. Considering this reaction at equilibrium, for the BaO-containing ternary slag, the chemical activity of BaO in the CaO-BaO-SiO_2 slag can be expressed as:

$$a_{BaO} = \left[\frac{a_{SiO2} {a_{Ba}}^2}{a_{Si}\, exp\left(\frac{-\Delta G^{\circ}_3}{RT}\right)} \right]^{\frac{1}{2}} \qquad (7)$$

The concentration of Ba in liquid silicon is low and dilute solutions of Ba in silicon are in contact with the slags containing low BaO concentrations. Assuming no significant interaction between dissolved Ba and Ca in silicon, we may calculate the chemical activities of Ba in silicon using the above calculated γ°_{Ba} for Ba in liquid silicon. On the other hand, as the concentration of BaO in the slags is low and $X_{BaO} < 0.034$ according to Table 1, it is a fair approximation to consider the thermodynamics data for binary CaO-SiO_2 slags to calculate the chemical activity of SiO_2 in the slags. Based on the activity data for SiO_2 in CaO-SiO_2 system by Rein and Chipman [26], which are reliable as compared with literature previously [27], a_{SiO2}

can be estimated around 0.8 and 0.85 at 1773 K (1500˚C) and 1873 K (1600˚C), respectively. Assuming the activity of silicon solvent as unity, we can calculate the chemical activity of BaO in the slag phases as shown in Fig. 10 for the two temperatures. The calculated results give $\gamma^{\circ}_{BaO} = 1.1 \times 10^{-4}$ and $\gamma^{\circ}_{BaO} = 17.8 \times 10^{-4}$ for the dilute solutions of BaO in CaO-SiO_2 slags at 1773 K (1500˚C) and 1873 K (1600˚C), respectively. It is worth mentioning that for the experiments 9 and 12 with no BaO in the slag, very low concentrations of Ba and BaO in the silicon and slag phases were measured in ppmw level, and Ba source is the trace impurity in the slag phase and this gave points in Figure 10 for very low BaO concentrations. The large difference between the activities of BaO at the two studied temperatures may indicate that there is interactions between the BaO, CaO and SiO_2 components in the slag phase, which are significantly dependent on temperature. Further precise work on this ternary slag system may provide more information to gain a better understanding of BaO thermochemical behavior in these slags.

4.3. Mass transport of Ca

As mentioned above, when silicon is contacted with the CaO-BaO-SiO_2 ternary slag, the partial silicothermic reduction of CaO from slag occurs through reaction (4) simultaneously with BaO reduction. As BaO is more readily reduced due to considerably larger K_3 value compared to K_4 value, i.e. 4000 larger at 1773 K (1500˚C), there will be larger extent of Ba transfer than Ca transfer from the slag into the melt, as seen in Fig. 3. In addition to reactions (3) and (4), the other reaction that can show equilibrium in the system regarding these components is:

$$\underline{Ca} + (BaO) = \underline{Ba} + (CaO) \qquad K_8 = (at\ 1773\ K) = 65.74 \qquad (8)$$

This reaction at equilibrium condition may yield:

$$\frac{X_{Ba}}{X_{Ca}} = \left(K_8 \frac{\gamma_{Ca}\gamma_{BaO}}{\gamma_{CaO}\gamma_{Ba}}\right)\frac{X_{BaO}}{X_{CaO}} \qquad (9)$$

The term in the parenthesis is a constant value for a given temperature and depending on the interaction between the slag components (CaO and BaO), Ba and Ca are distributed. The slope of the lines in Fig. 3 may show the magnitude of the term in parenthesis in Eq. (9) and as we see more extent of Ca transfer into the melt (relative to Ba transfer) occurs at higher temperatures. Although the reaction constant K_8 decreases with increasing temperatures, the most important parameter for Ca and Ba distribution will be the structure of the slag and the corresponding interactions between CaO and BaO in it, appeared in their activity coefficient terms in Eq. (9).

4.4. Phosphorous distribution thermochemistry

Although a couple of chemical reactions may occur for the oxidation of the dissolved P in silicon or the reduction of its oxide from the slag, the equilibrium can be studied considering the following reaction for the both $BaO\text{-}SiO_2$ and $CaO\text{-}BaO\text{-}SiO_2$ slags:

$$4\,\underline{P} + 5\,(SiO_2) = 2\,(P_2O_5) + 5\,Si \qquad K_{10}\,(at\ 1773\ K) = 4.15 \times 10^{-46} \qquad (10)$$

Considering the equilibrium for reaction (10), we obtain the following expression for the chemical activity of P_2O_5 in the slag:

$$a_{P2O5} = \left[\frac{{a_{SiO_2}}^5 {a_P}^4}{{a_{Si}}^5} K_{10}\right]^{\frac{1}{2}} \quad (11)$$

The chemical activity of P in liquid silicon, a_P, can be calculated for different measured chemical compositions considering the phosphorous activity coefficients as $\gamma_P^\circ = 0.47$ and $\gamma_P^\circ = 0.49$ at 1500˚C and 1600˚C, respectively.[28] Activities of SiO_2 in the slags for the given chemical compositions at equilibrium in Table 1 can be determined by the outlined approach above for BaO-SiO_2 slags and the literature data for low BaO-containing CaO-SiO_2 slags. [22-25] Employing the HSC Chemistry thermodynamic software for calculating the changes in the reaction constant, K_{10}, the activity of P_2O_5 can be calculated for the both types of slags as shown against the P_2O_5 molar fraction in Fig. 11.

The calculated activities for P_2O_5 in the slags can be used to determine the activity coefficient of dilute solutions of P_2O_5 in the slags. This yields $\gamma_{P2O5}^\circ = 2 \times 10^{-32}$ and $\gamma_{P2O5}^\circ = 1 \times 10^{-30}$ for illustrated system in Figure 11 for BaO-SiO_2 slags at 1500˚C and 1600˚C, respectively. Similarly for low BaO containing CaO-SiO_2 slags at 1773 K (1500˚C) and 1873 K (1600˚C), $\gamma_{P2O5}^\circ = 4 \times 10^{-33}$ and $\gamma_{P2O5}^\circ = 3 \times 10^{-31}$ are obtained, respectively. Although these very small activity coefficients for P_2O_5 in the slags are obtained, not significant phosphorous is removed from silicon into the slag, which is due to the very small reaction constant for chemical reaction (10).

The other type of chemical reaction for P transport from silicon to the adjacent slag is the formation of barium phosphide according to the following reaction:

$$2\,\underline{P} + 3\,\underline{Ba} = Ba_3P_2 \qquad K_{12}\ (at\ 1773\ K) = 3.7 \times 10^5 \qquad (12)$$

The chemical activity of Ba_3P_2 in the slags can be calculated using the above calculated chemical activities for P and Ba and this yields larger activities for this compound compared to the calculated P_2O_5 activities. This may indicate that the formation of P_2O_5 is a more stable form than Ba_3P_2 in the slag. However, in order to study the thermodynamics of P removal from silicon in BaO-SiO_2 system through these mechanisms, the following overall chemical reaction can be considered:

$$Ba_3P_2 + 4(SiO_2) = 3(BaO) + (P_2O_5) + 4Si \qquad K_{13}\ (at\ 1773\ K) = 1.6 \times 10^{-21} \qquad (13)$$

Considering the equilibrium constant for this reaction, K_{13}, we may write:

$$\left(\frac{a_{P2O5}}{a_{Ba3P2}}\right)_{eq} = \frac{K_{13}{a_{SiO2}}^4}{{a_{BaO}}^3{a_{Si}}^4} \qquad (14)$$

Based on the above calculated chemical activities for SiO_2 and BaO and considering Raoultian behavior for silicon, the right part of Eq. (14) can be calculated as illustrated in Figure 12 for two temperatures. It is found observed that for all the experiments $\left(\frac{a_{P2O5}}{a_{Ba3P2}}\right) < \left(\frac{a_{P2O5}}{a_{Ba3P2}}\right)_{eq}$, indicating that P_2O_5 is the more stable P-containing phase in the slag. Therefore, we may conclude that the mechanism of P adsorption into the slag is through the chemical reaction (10).

The distribution of P, and in another word, the extent of P transfer between the two phases is depending on the type of slag as observed in Figs. 4 and 5. Considering chemical reaction (10), the formation of P_2O_5 is in relation with the source of oxygen in the system (SiO_2), and therefore there must be a higher rate of P oxidation from silicon for lower basicity. For a given slag composition, observing lower L_P value at higher temperature is attributed to the increase of P_2O_5 activity in the slag, while the activity of P in liquid silicon is not significantly changed by temperature change. On the other hand, the value of L_P is dependent on the basicity and the structure of slag and as P_2O_5 is an acidic agent in the slag, L_P is expected to be increased with increasing basicity. This is observed for the BaO-SiO_2 slag, while it is less dependent on basicity for CaO-BaO-SiO_2 at 1873 K (1600˚C). However, it is hard to explain the observed not significant L_P dependent on basicity for the other conditions in this study. The L_P values in Figs. 4 and 5 for calcium-silicate slags are obviously larger than barium-silicate slags. This may be explained considering the affinity of the acidic agent P_2O_5 in the slags with the main basic components as it can be in the form of calcium phosphates of $CaO\cdot P_2O_5$ and $3CaO\cdot P_2O_5$, or barium phosphate of $3BaO\cdot P_2O_5$. The main chemical reactions for the formation of these components can be written as:

$$CaO+P_2O_5= CaO\cdot P_2O_5 \qquad K_{15}\,(at\ 1773\ K) = 2.03\times10^{8} \qquad (15)$$

$$3CaO+P_2O_5= 3CaO\cdot P_2O_5 \qquad K_{16}\,(at\ 1773\ K) = 2.07\times10^{19} \qquad (16)$$

$$3BaO+P_2O_5= 3BaO\cdot P_2O_5 \qquad K_{17}\,(at\ 1773\ K) = 5.53\times10^{8} \qquad (17)$$

The magnitude of the reaction constants K_{15}, K_{16}, and K_{17} indicates that for the slags in experiments 9 to 14, where CaO is the main basic component, we may have a better affinity of P_2O_5 in the slag through the formation of $3CaO\cdot P_2O_5$ compared to barium silicate slags, which is observed in significantly higher L_P-values for CaO-(BaO)-SiO_2 slags compared to BaO-SiO_2 slags (Figs. 4 and 5).

4.5. Chemical activity of boron oxide

It is generally accepted in literature that boron exists in the silicate slags in the form of oxide B_2O_3. As there is always significant amount of silicon oxide in the slag in contact with liquid silicon, the equilibrium can be studied considering the following reaction for the both studied binary and ternary silicate slags:

$$2\,\underline{B} + 3/2\,(SiO_2) = (B_2O_3) + 3/2\,Si \qquad K_{18}\,(at\ 1773\ K) = 9.3\times10^{-2} \qquad (18)$$

and the chemical activity of B_2O_3 at equilibrium can be expressed as:

$$a_{B2O3} = \frac{{a_{SiO2}}^{3/2}{a_B}^2}{{a_{Si}}^{3/2}}\,K_{18} \qquad (19)$$

The chemical activity of B in molten silicon can be calculated using the data literature, [29] which yields $\gamma_B^\circ = 3.87$ and $\gamma_B^\circ = 3.65$ at 1773 K (1500˚C) and 1873 K (1600˚C), respectively. It is a fair approximation to consider Raoutian behavior for silicon solvent, and we can consider a_{Si} equal to its molar faction, which is close to unity. Employing the HSC Chemistry thermodynamic software for calculating the changes in the reaction constant, K_{18}, the activity of B_2O_3 can be calculated for the both types of slags as presented against the B_2O_3 concentration in Fig. 13 for typical conditions. The calculations here yield the following expressions for the activity coefficient of B_2O_3 in specific BaO-SiO_2 slags at different temperatures:

$$ln\gamma_{B2O3}(at\ 1773\ K) = 7\times10^{-10} + 0.554X_{B2O3} + 0.48{X_{B2O3}}^2 \qquad (20)$$

$$ln\gamma_{B2O3}(at\ 1873\ K) = 2\times10^{-9} + 1.39X_{B2O3} + 0.62{X_{B2O3}}^2 \qquad (21)$$

For the above expressions $L_B=1$ was considered, which is a fair approximation (Fig. 6) and the calculations for the experimental points are well correlated in Fig. 13. Similarly, the following expressions are obtained for low BaO-containing CaO-BaO-SiO_2:

$$ln\gamma_{B2O3}(at\ 1773\ K) = 7 \times 10^{-9} + 0.23X_{B2O3} + 0.246{X_{B2O3}}^2 \quad (22)$$

$$ln\gamma_{B2O3}(at\ 1873\ K) = 1 \times 10^{-8} + 0.51X_{B2O3} + 0.543{X_{B2O3}}^2 \quad (23)$$

It is worth noting that the activity coefficient of B_2O_3 is not significantly affected by L_B changes and close γ_{B2O3} values are obtained for different L_B-*values* by Eqs. (20)-(23). These equations show higher activity coefficients for boron oxide in the BaO-SiO_2 slags than CaO-BaO-SiO_2 slags, which may indicate the higher affinity of boron into CaO-SiO_2 slags which causes the significantly higher L_B value for these slags as observed through comparing Figs. 6 and 7.

4.6. Boron removal mechanism

When a boron-containing silicon melt is contacted with a BaO-SiO_2 slag, the oxidation of the dissolved boron occurs, assuming smaller initial B_2O_3 than equilibrium concentration in the slag. The oxidation can occur via the chemical reaction (18) or via the following reaction:

$$2\ \underline{B} + 3(BaO) = (B_2O_3) + 3\ \underline{Ba} \qquad K_{24}\ (at\ 1773\ K) = 3.18\times10^{-9} \quad (24)$$

Calculating the changes in the standard Gibbs energy for chemical reactions (18) and (24), ΔG°_{18} and ΔG°_{24}, we find that pure oxides of Si and Ba are stable in contact with pure B. However, when BaO-SiO_2 slag containing is contacted with the liquid silicon containing small amounts of B, the mass transfer of B from silicon into the slag occurs due to the very small

activity coefficient of B_2O_3 in the slag. We can determine the reaction mechanism for B oxidation through calculating the changes in Gibbs energy of reactions (18) and (24):

$$\Delta G_{18} = \Delta G^{\circ}_{18} + RTln\left(\frac{a_{B2O3}{a_{Si}}^{3/2}}{{a_B}^2{a_{SiO2}}^{3/2}}\right) \quad (25)$$

$$\Delta G_{24} = \Delta G^{\circ}_{24} + RTln\left(\frac{a_{B2O3}{a_{Ba}}^{3}}{{a_B}^2{a_{BaO}}^{3}}\right) \quad (26)$$

In order to find out the reaction with lower Gibbs energy independent of the concentrations of B and B_2O_3 in the two phases, we can obtain the following equations by rearranging the above equations:

$$F_{18} = \Delta G_{18} - RTln\left(\frac{a_{B2O3}}{{a_B}^2}\right) = \Delta G^{\circ}_{18} + RTln\left(\frac{{a_{Si}}^{3/2}}{{a_{SiO2}}^{3/2}}\right) \quad (27)$$

$$F_{24} = \Delta G_{24} - RTln\left(\frac{a_{B2O3}}{{a_B}^2}\right) = \Delta G^{\circ}_{24} + RTln\left(\frac{{a_{Ba}}^{3}}{{a_{BaO}}^{3}}\right) \quad (28)$$

Obviously, the magnitude of F_{18} and F_{24} for given process conditions will show that which chemical reaction occurs for B oxidation from thermodynamics point of view; the reaction with lower *F-value*. Figure 14 shows the calculated F_{18} and F_{24} values for different given Ba concentrations in silicon and for a wide composition range of BaO-SiO_2 slags at 1773 K (1500˚C) and 1873 K (1600˚C) using the above determined activities for the involved species. As seen, for a large slag composition range up to 60% SiO_2 and up to 0.04 wt% Ba in silicon the chemical reaction (24) is the dominant reaction for B removal. However, for the high SiO_2

concentrations and when high concentrations of Ba in silicon is maintained, the chemical reaction (18) may be the mechanism for B removal. For the experiments 1 to 8 the initial slags are in the range of X_{SiO2}=0.63 to 0.76 and after the reaction the slags contain X_{SiO2}=0.66 to 0.78. Therefore, we may conclude that at initial the B removal occurs by chemical reaction (24) and after reaching a specific level of Ba in silicon, the further B removal occurs by chemical reaction (18). However, for some experiments with small Ba transfer to silicon, only the chemical reaction (24) is the one involved in B oxidation.

5. Conclusions

The interactions of B- and P-doped silicon with BaO-SiO_2 slags and low BaO containing CaO-BaO-SiO_2 at 1773 K (1500˚C) and 1873 K (1600˚C) were studied, and the main conclusions for our temperature and compositions can be summarized as:

- The distribution coefficient of B for BaO-SiO_2 slags is L_B=*2.2±0.2*, which is higher than that for low BaO-containing CaO-SiO_2 slags (L_B=*1.1±0.2*), and L_B is not significantly affected by temperature and composition changes of the slags.
- The distribution coefficient of P, L_P, is in the ranges of 0.25-0.7, which is significantly smaller than L_B. However, L_P is higher for BaO-SiO_2 slags than that for low BaO-containing CaO-SiO_2 slags, and L_P is higher at lower temperatures.
- The mass transfer of Ba from slag into liquid silicon occurs through silicothermic reduction, which causes dilute solutions of Ba in silicon, and the temperature dependence of the activity coefficient of Ba in silicon can be presented by Eq. (6).
- The mass transport of P from silicon into the silicate slags is through oxidation by SiO_2 and the formation of P_2O_5 is dominant compared to formation of Ba_3P_2. Although very small chemical activity for P_2O_5 in slags is calculated, P is not significantly removed from silicon.

- Boron is removed from silicon through oxidation by BaO from the slag at high BaO concentrations and until the Ba concentration in silicon reaches an specific concentration. Further B removal occurs through oxidation by SiO_2 in the slag.

Acknowledgement

The present research has been supported by Research Domain 5–Materials and Society in SFI Metal Production (a Norwegian Centre for Research-driven Innovation in metal production) through project number 237738.

References

[1] Schei A, Tuset J.Kr, Tveit H (1998): *Production of high silicon alloys*. Trondheim, Tapir Forlag.

[2] Braga AFB, Zampieri PR, Bacchin JM, Mei PR (2008) Review: New processes for the production of solar-grade polycrystalline silicon, Solar Energy Materials & Solar Cells, 92: 418-424.

[3] Safarian J, Tranell G, Tangstad M (2012) Processes for upgrading metallurgical grade silicon to solar grade silicon, Energy Procedia, 20: 88-97.

[4] Hopkins RH, Rohatgi A: (1986) Impurity effects in silicon for high efficiency solar cells, J. Cryst. Growth, 75: 67-79.

[5] Liaw HM, Secco D'Aragona F (1983) Purification of metallurgical-grade silicon by slagging and impurity redistribution, Solar Cells, 10:109-118.

[6] Suzuki K, Sugiyama T, Takano K, Sano N (1990) Thermodynamics for removal of boron from metallurgical silicon by flux treatment, J. Jpn. Inst. Met. 54**:** 168 – 172.

[7] Weiss T, Schwerdtfeger K (1994) Chemical equilibria between silicon and slag melts, Met. Mat. Trans. B, 25b: 497-504.

[8] Teixeira LAV, Tokuda Y, Yoko T, Morita K (2009) Behaviour and state of boron in CaO-SiO_2 slags during refining of solar grade silicon, ISIJ Int., 49: 777-782.

[9] Jakobsson LK, Tangstad M (2012) Distribution of boron and calcium between silicon and calcium silicate slags, International Smelting Technology Symposium (Incorporating the 6th Advances in Sulfide Smelting Symposium**)**, Ed. J. P. Downey, T.P. Battle, J.F. White, TMS 2012: 179-184.

[10] Krystad E, Tang K, Tranell G (2012) The kinetics of boron removal transfer in slag refining of silicon,JOM, 64: 968-972.

[11] Dietle J (1987) Metallurgical ways of silicon meltstock processing. In: Silicon for Photovoltaics, 2: 285–352.

[12] Cai J,.Li JT, Chen WH, Chen C, Luo XT (2011) Boron removal from metallurgical silicon using CaO-SiO_2-CaF_2 slags, Trans. Nonferrous Met. Soc. China, 21: 1402-1406.

[13] White J, Allertz C, Forwald K, Sichen D (2013) The thermodynamics of boron extraction from liquid silicon using SiO_2-CaO-MgO slag treatment, Int. J. Materials Research, 104: 229-234.

[14] Luo DW, Liu N, Lu YP, Zhang GL, Li TJ: Removal of boron from metallurgical grade silicon by electromagnetic induction slag melting, Trans. Nonferrous Met. Soc. China, 21: 1178-1184.

[15] Tanahashi M, Shinpo Y, Fujisawa T Yamauchi C (2002) Distribution behaviour of boron between SiO2 saturated NaO0.5-CaO-SiO_2 flux and molten silicon, J. Min. Mat. Proc. Inst. Japan, 118: 497-505.

[16] Johnston MD, Barati M (2010) Distribution of impurity elements in slag-silicon equilibria for oxidative refining of metallurgical silicon for solar cell applications, Solar Energy Materials & Solar Cells, 94: 2085-2090.

[17] Safarian J, Tranell G, and Tangstad M (2013) Thermodynamic and kinetic behaviour of B and Na through the contact of B-doped silicon with Na_2O-SiO_2 slags, Metall. Mater. Trans. B, 44B:571–83.

[18] Safarian J, Tranell G, Tangstad M (2015) Boron removal from silicon by CaO-Na_2O-SiO_2 slags : Metall. Mater. Trans. E, 2E: 109-118.

[19] Safarian J, Tang K, Olsen JE, Andersson S, Tranell G, Hildal K (2016) Mechanisms and kinetics of boron removal from silicon by humidified hydrogen, Metall. Mater. Trans. B. 47B: 1063-1079.

[20] Safarian J, Tangstad M (2011) Phase diagram study of the Si-P system in Si-rich region, J. Mater. Res., 26: 1494-1503.

[21] Safarian J, Kolbeinsen L, Tangstad M (2012) Thermodynamic activities in silicon binary melts, J. Mater. Sci.,. 47: 5561-5580.

[22] Zhang R, Mao H, Taskinen P (2016) Thermodynamic descriptions of the BaO-CaO, BaO-SrO, BaO-SiO_2 systems, CALPHAD: Computer coupling of phase diagrams and thermochemistry, 54: 107-116.

[23] Tyurnina ZG, Lopatin SI, Shugurov SM, Stolyarova VL (2006) Thermodynamic properties of silicate glasses and melts, I. System BaO-SiO_2, Russian Journal of General Chemistry, vol. 76: 1522-1530.

[24] Tyurnina ZG, Stolyarova VL, Lopatin SI, Plotnikov EN (2006) Mass spectrometric investigation of the vaporization and thermodynamic properties of components in the BaO-SiO_2 system, Glass Physics and Chemistry, vol. 32: 533-542.

[25] Boulay E, Nakano J, Turner S, Idrissi H, Schryvers D, Godet S (2014) Critical assessment and thermodynamic modeling of BaO-SiO_2 and SiO_2-TiO_2 systems and their extensions into liquid immiscibility in the BaO-SiO_2-TiO_2 system, CALPHAD: Computer coupling of phase diagrams and thermochemistry , vol. 47: 68-82.

[26] Rein RH, J. Chipman J (1965) Activities in the liquid solution SiO_2-CaO-MgO-Al_2O_3 at 1600˚ Trans. Metall. Soc. AIME, 233: 415-425.

[27] Jakobsson LK (2013) Distribution of boron between silicon and CaO-SiO_2, MgO-SiO_2, CaO-MgO-SiO_2, and CaO-Al_2O_3-SiO_2 slags at 1600˚C, PhD thesis, NTNU, vol. 2013:326.

[28] Safarian J, Tangstad M (2012) Vacuum refining of molten silicon, Metall. Mater. Trans. B, 43B: 1427-1445.

[29] Yoshikawa T, Morita K (2005) Thermodynamic property of B in molten Si and phase relations in the Si-Al-B system, Mater. Trans., 46: 1335-1340.

Table Captions:

Table 1: The experimental conditions for interacting silicon and slag, and slag compositions before and after reaction.

Experiment no.	Temperature (˚C)	Initial slag compositions (wt%)			Final slag compositions (wt%)		
		BaO	CaO	SiO_2	BaO	CaO	SiO_2
1	1500	45.01	0	54.95	42.6	0	57.4
2	1500	49.6	0	50.2	45	0	55
3	1500	55.03	0	44.93	49.5	0	50.5
4	1500	60.04	0	39.95	56.8	0	43.2
5	1600	45.05	0	54.92	41.4	0	58.6
6	1600	50.03	0	49.95	44.8	0	55.2
7	1600	55.1	0	44.9	49.0	0	51.0
8	1600	60.01	0	39.94	53.4	0	46.6
9	1500	0	40.05	59.9	0	40.0	60.0
10	1500	2.5	39.0	58.5	2.5	38.9	58.6
11	1500	4.95	38.05	57.0	4.9	37.95	57.15
12	1600	0	40.02	59.93	0	39.9	60.05
13	1600	5.01	37.95	57.03	4.6	35.3	60.1
14	1600	10.02	36.05	53.91	8.6	33.9	57.5

Figure Captions:

Figure 1: Relationship between Ba concentration in silicon and the basicity of $BaO\text{-}SiO_2$ slags.

Figure 2: Relationship between Ba concentration in silicon and the basicity of CaO-(BaO)-SiO_2 slags.

Figure 3: Relationship between X_{Ba}/X_{Ca} ratio in silicon and the X_{BaO}/X_{SiO2} in CaO-(BaO)-SiO_2 slags at equilibrium, X_i denotes molar fraction of component *i*.

Figure 4: L_P-value changes with basicity of $BaO\text{-}SiO_2$ slags at different temperatures.

Figure 5: L_P-value changes with basicity of CaO-BaO-SiO_2 slags at different temperatures.

Figure 6: L_B-value changes with basicity of $BaO\text{-}SiO_2$ slags at different temperatures.

Figure 7: L_B-value changes with basicity of CaO-BaO-SiO_2 slags at different temperatures.

Figure 8: Chemical activities of $BaO\text{-}SiO_2$ slags components at different temperatures.

Figure 9: Chemical activities of dilute solutions of Ba in silicon.

Figure 10: Chemical activities of dilute solutions of BaO in CaO-BaO-SiO_2 slags.

Figure 11: Calculated chemical activities of dilute solutions of P_2O_5 in $BaO\text{-}SiO_2$ and CaO-BaO-SiO_2 slags at given representative conditions, symbols: calculated using experimental data.

Figure 12: Relationship between $\left(\frac{a_{P2O5}}{a_{Ba3P2}}\right)_{eq}$ and composition of $BaO\text{-}SiO_2$ slags in equilibrium with silicon containing low P concentrations, symbols: calculated using experimental data.

Figure 13: Calculated chemical activities of dilute solutions of B_2O_3 in $BaO\text{-}SiO_2$ and $CaO\text{-}BaO\text{-}SiO_2$ slags at representative equilibrium conditions, , symbols: calculated using experimental data.

Figure 14: Calculated changes of F_{18} and F_{24} functions with $BaO\text{-}SiO_2$ slags compositions for different temperatures and Ba concentrations in silicon.

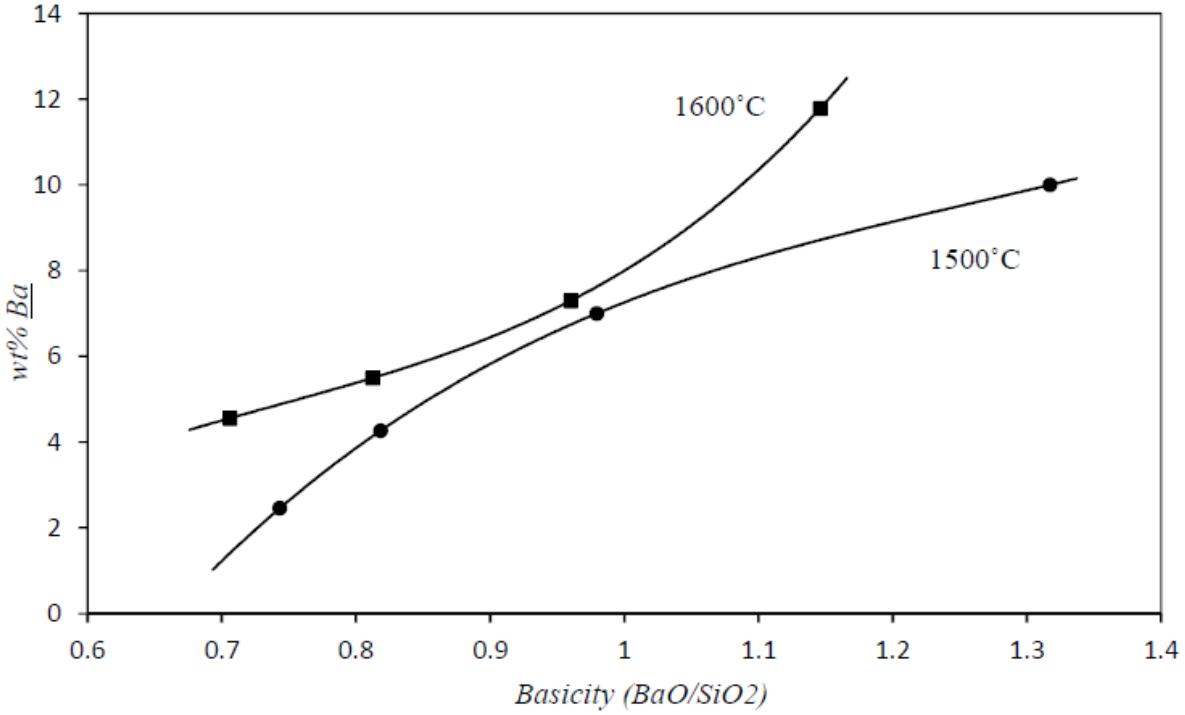
14
12
10
8
6
4
2
0
0.6
0.7
0.8
0.9
1
1.1
1.2
1.3
1.4
1600˚C
1500˚C
wt% Ba
Basicity (BaO/SiO2)

Fig. 1

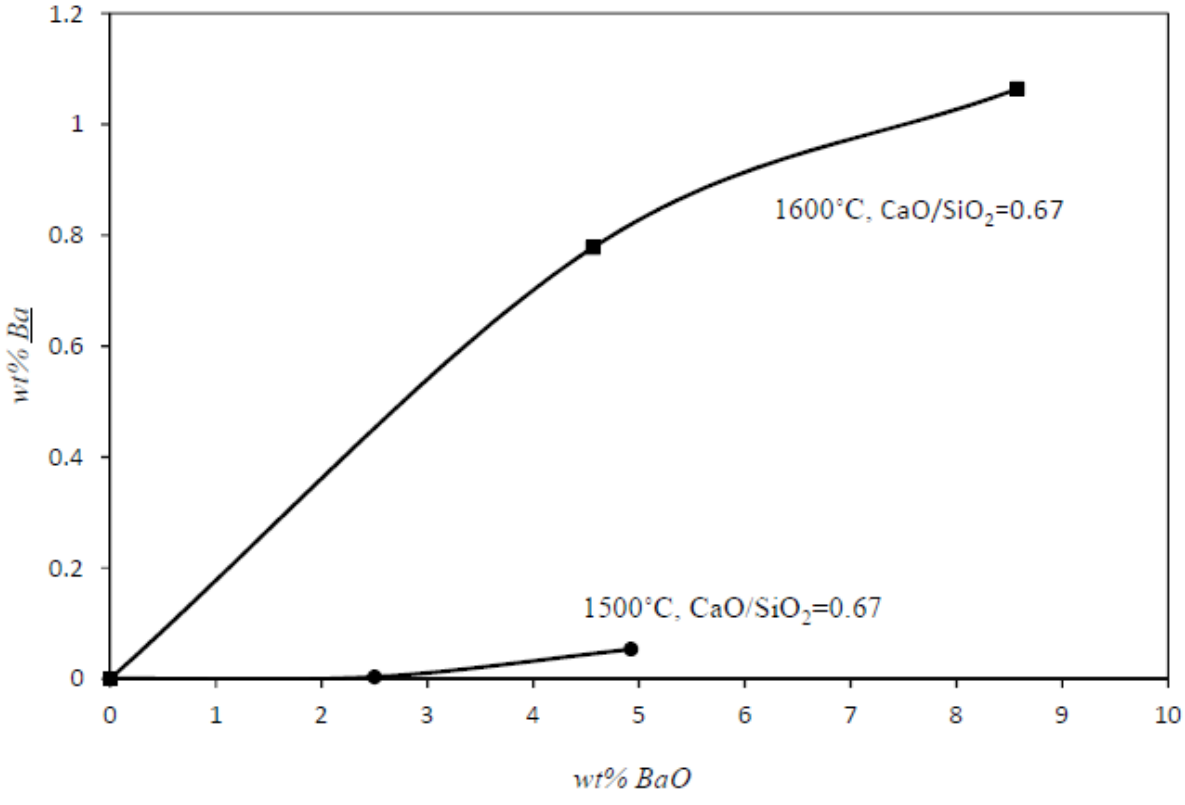
1.2
1
0.8
0.6
0.4
0.2
0
0
1
2
3
4
5
6
7
8
9
10
1600˚C, CaO/SiO2=0.67
1500˚C, CaO/SiO2=0.67
wt% Ba
wt% BaO

Fig. 2

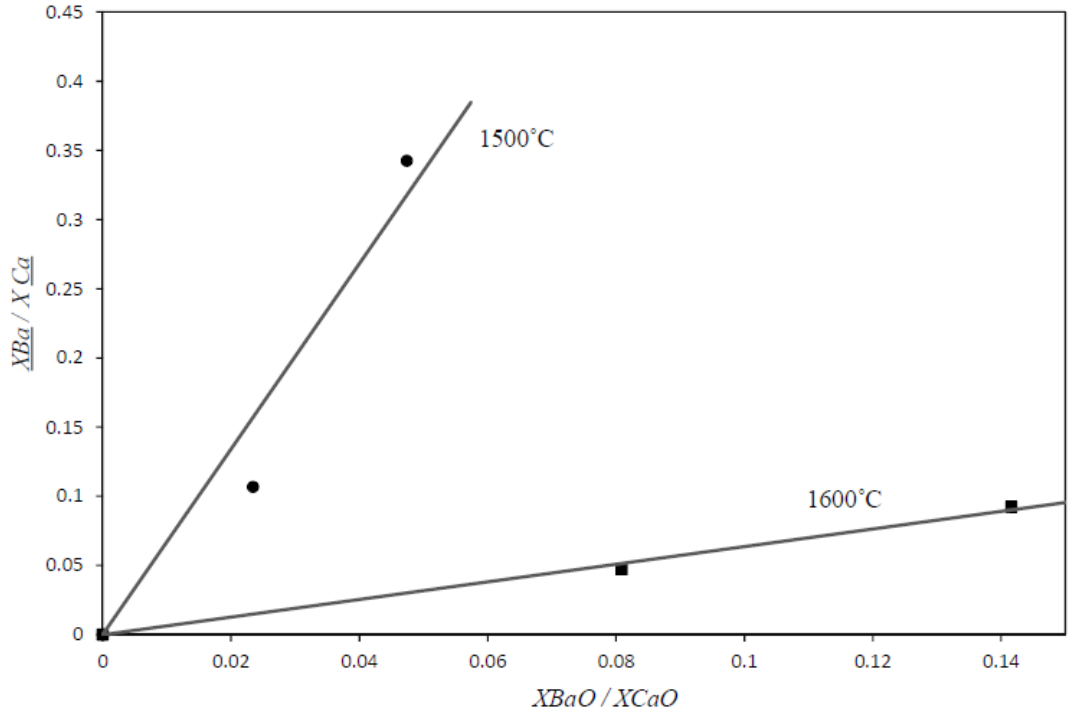
0.45
0.4
0.35
0.3
0.25
0.2
0.15
0.1
0.05
0
XBa / X Ca
1500˚C
1600˚C
0
0.02
0.04
0.06
0.08
0.1
0.12
0.14
XBaO / XCaO

Fig. 3

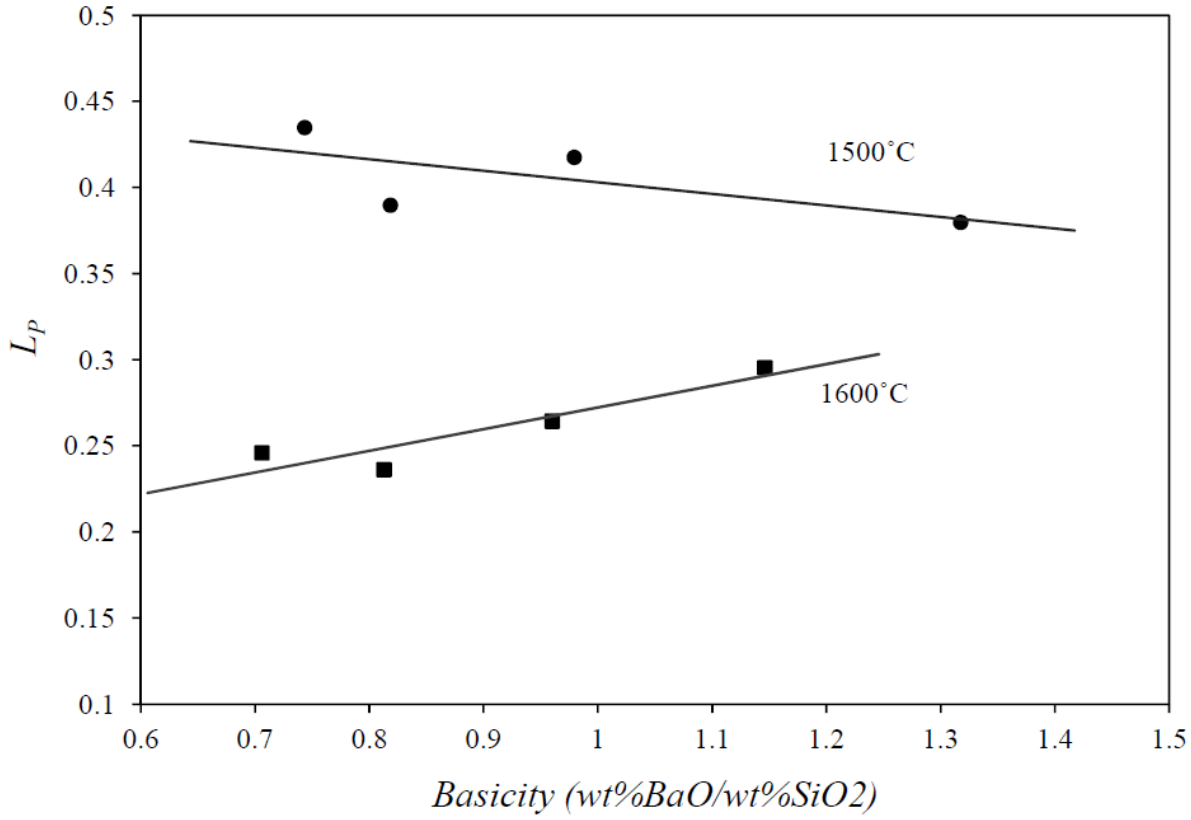
0.5
0.45
0.4
0.35
0.3
0.25
0.2
0.15
0.1
L_P
1500˚C
1600˚C
0.6
0.7
0.8
0.9
1
1.1
1.2
1.3
1.4
1.5
Basicity (wt%BaO/wt%SiO2)

Fig. 4

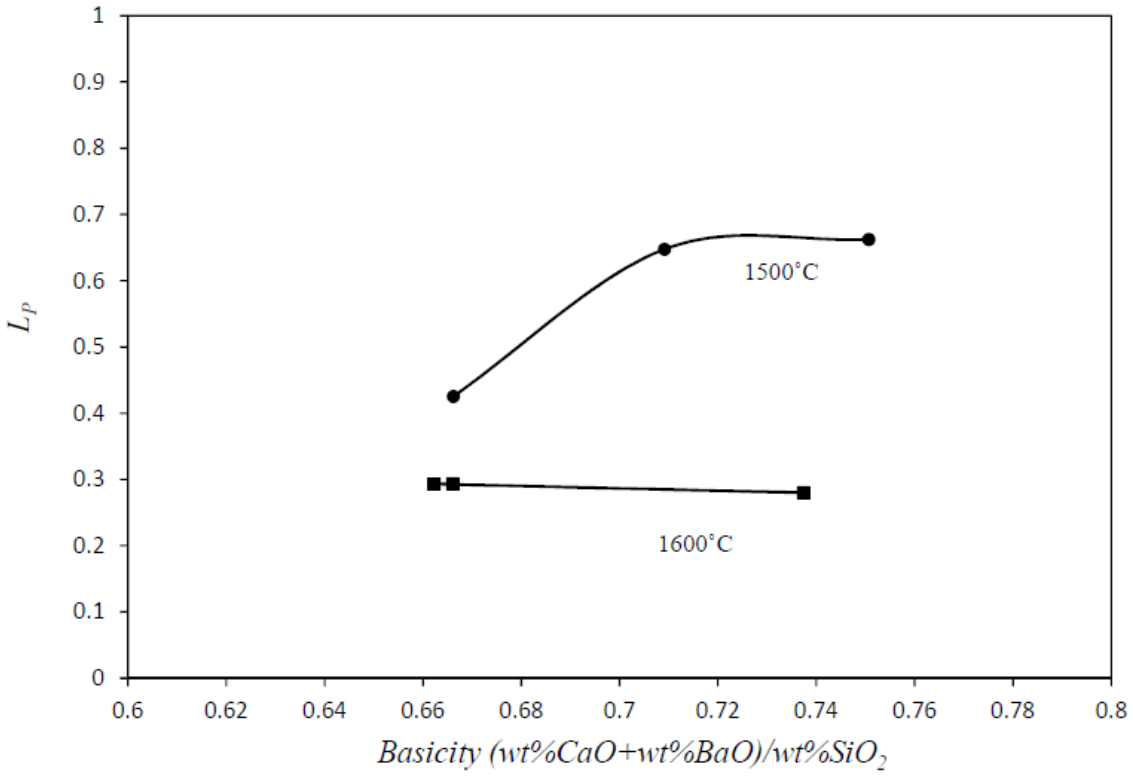

Fig. 5

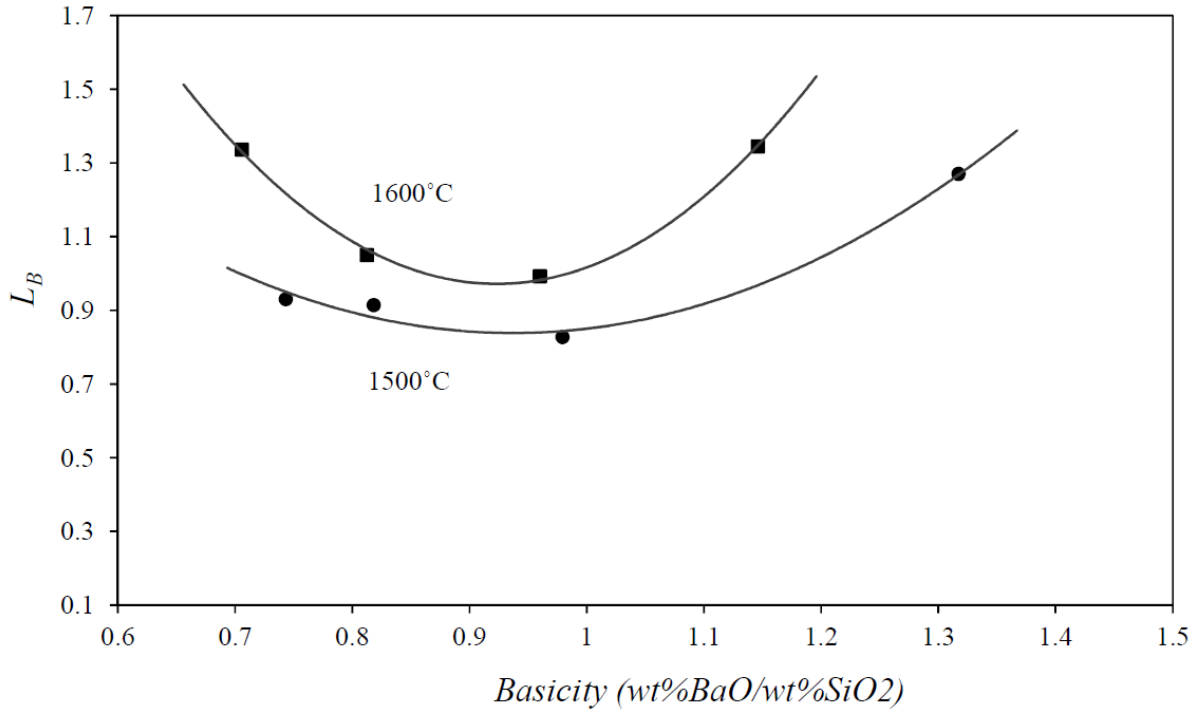

Figure 6

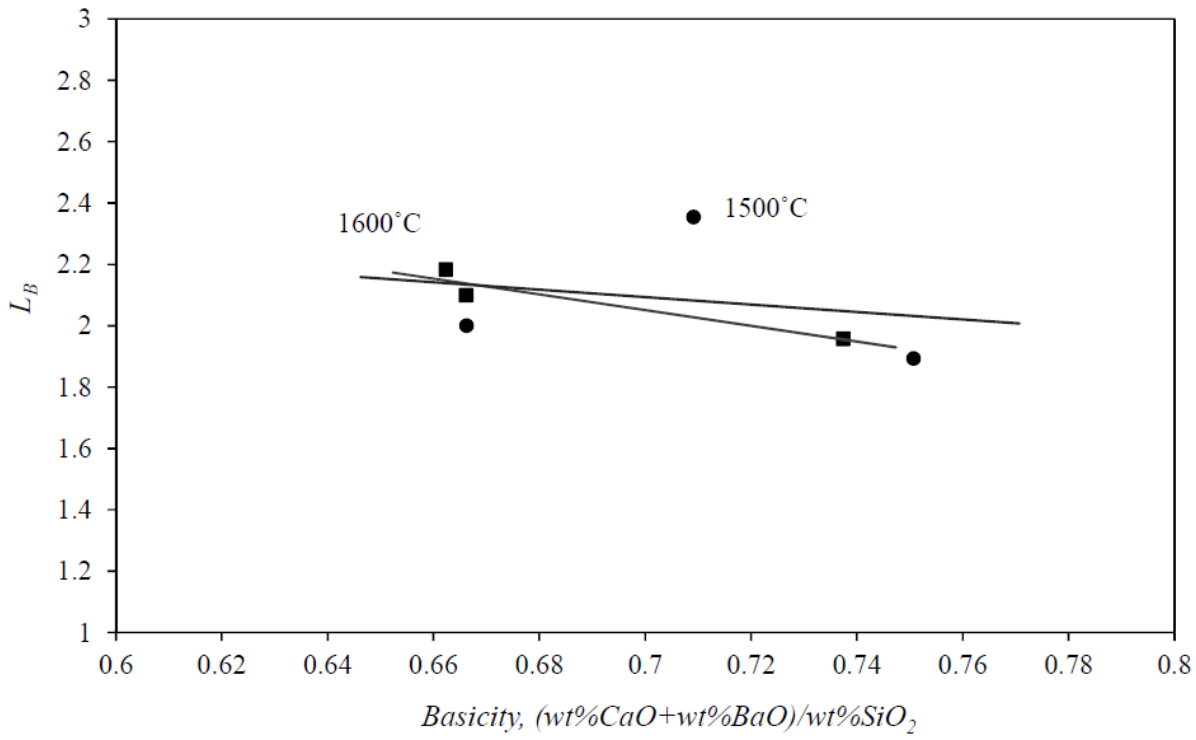
1600˚C
1500˚C
L_B
Basicity, (wt%CaO+wt%BaO)/wt%SiO_2

Fig. 7

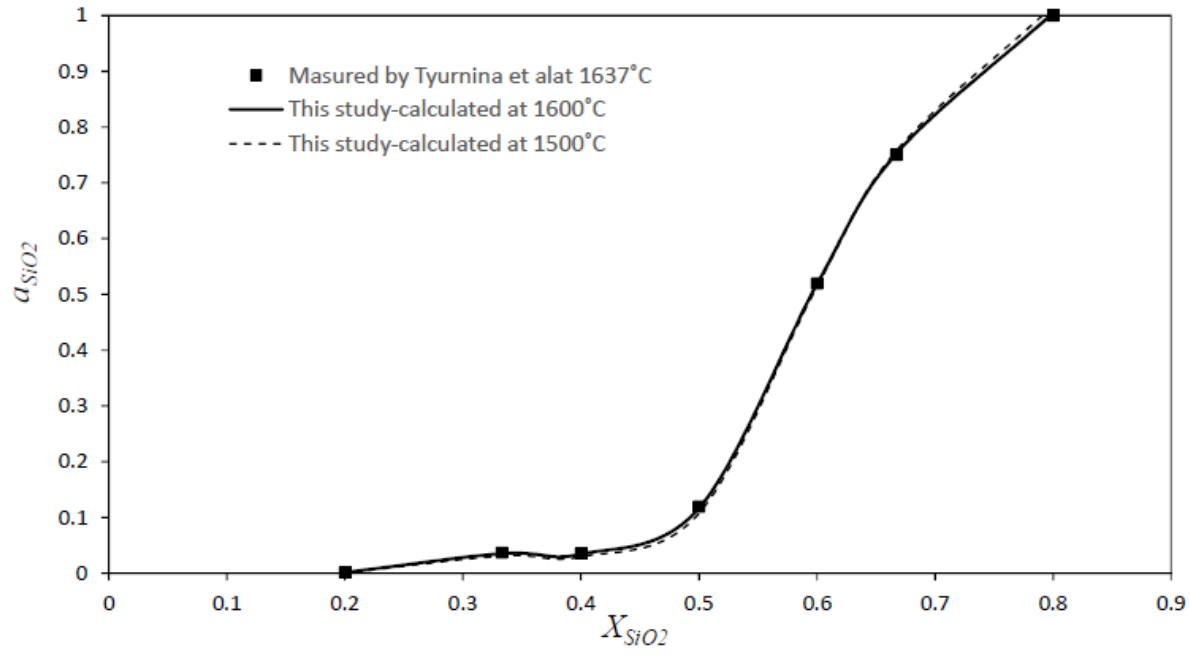
Masured by Tyurnina et alat 1637˚C
This study-calculated at 1600˚C
This study-calculated at 1500˚C
a_{SiO2}
X_{SiO2}

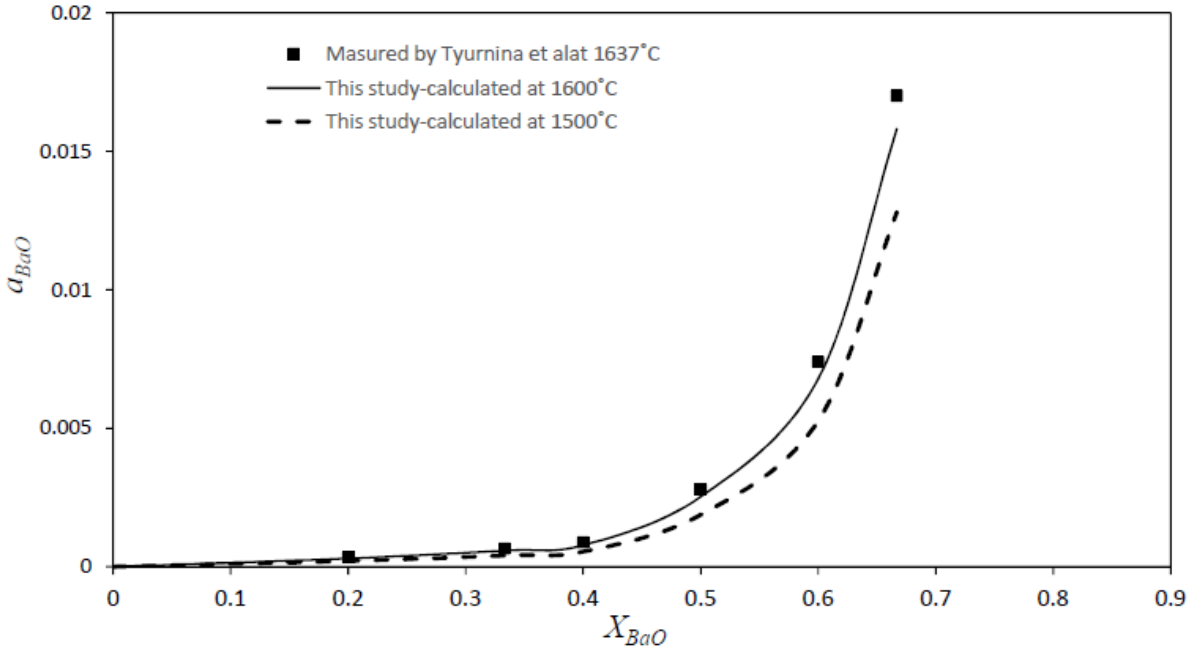
Masured by Tyurnina et alat 1637˚C
This study-calculated at 1600˚C
This study-calculated at 1500˚C
a_{BaO}
X_{BaO}
0.02
0.015
0.01
0.005
0
0
0.1
0.2
0.3
0.4
0.5
0.6
0.7
0.8
0.9

Fig. 8

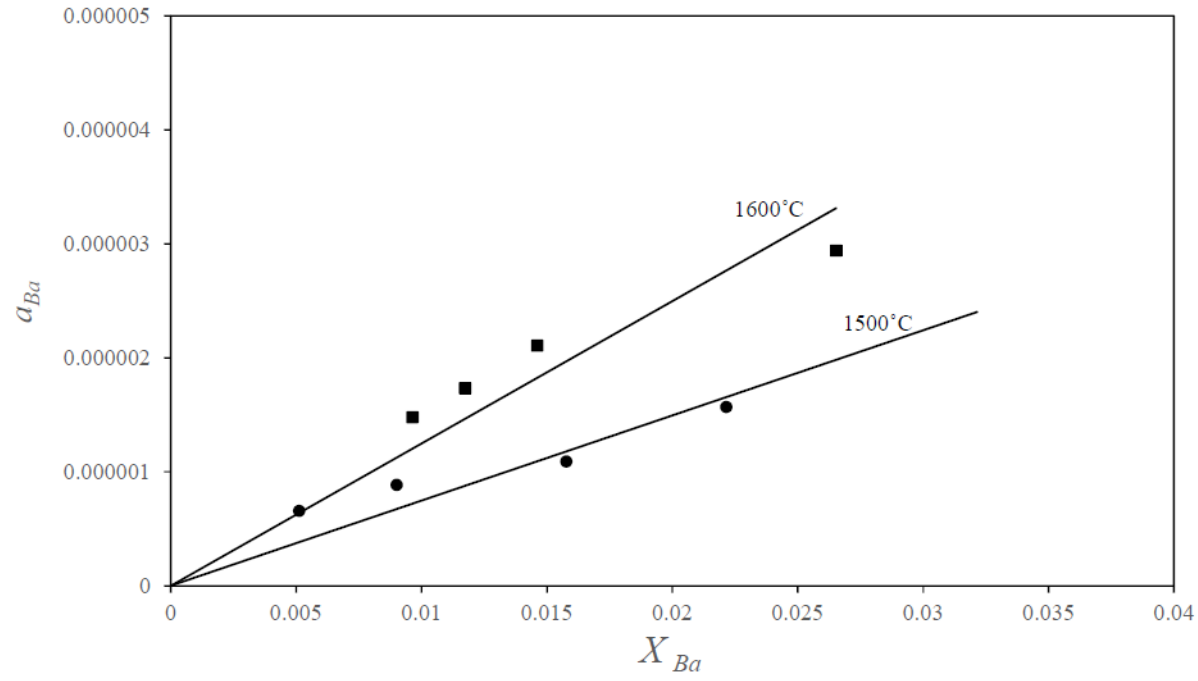
1600˚C
1500˚C
a_{Ba}
X_{Ba}
0.000005
0.000004
0.000003
0.000002
0.000001
0
0
0.005
0.01
0.015
0.02
0.025
0.03
0.035
0.04

Fig. 9

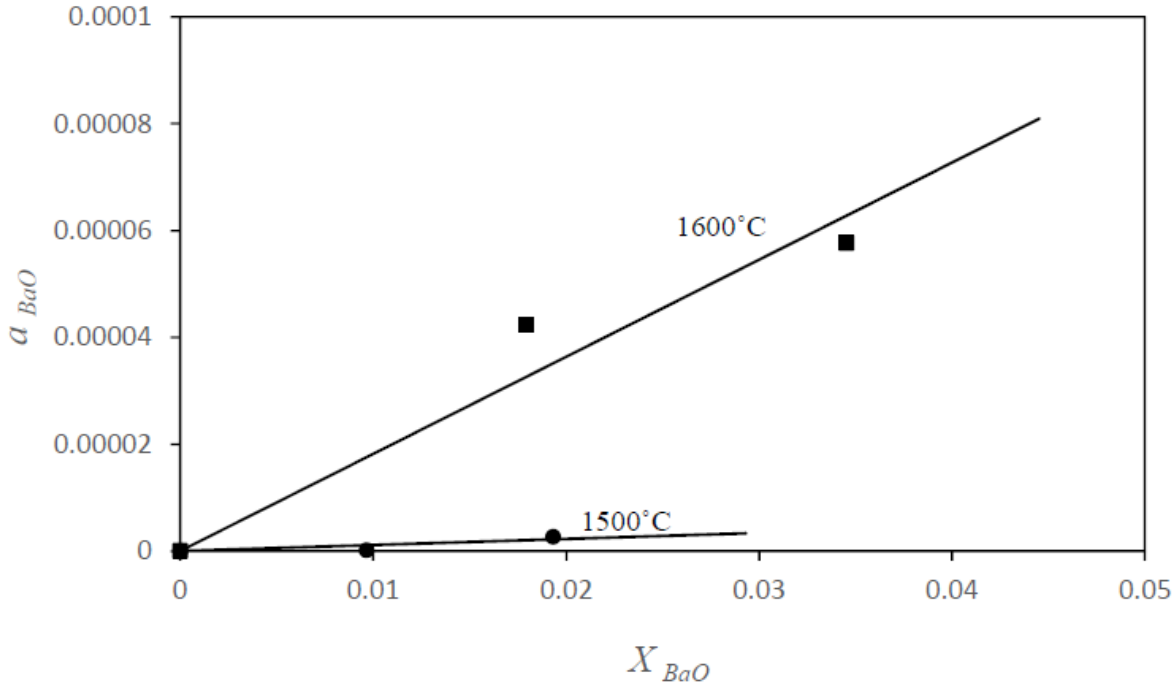
0.0001
0.00008
0.00006
0.00004
0.00002
0
a_{BaO}
1600°C
1500°C
0
0.01
0.02
0.03
0.04
0.05
X_{BaO}

Fig. 10

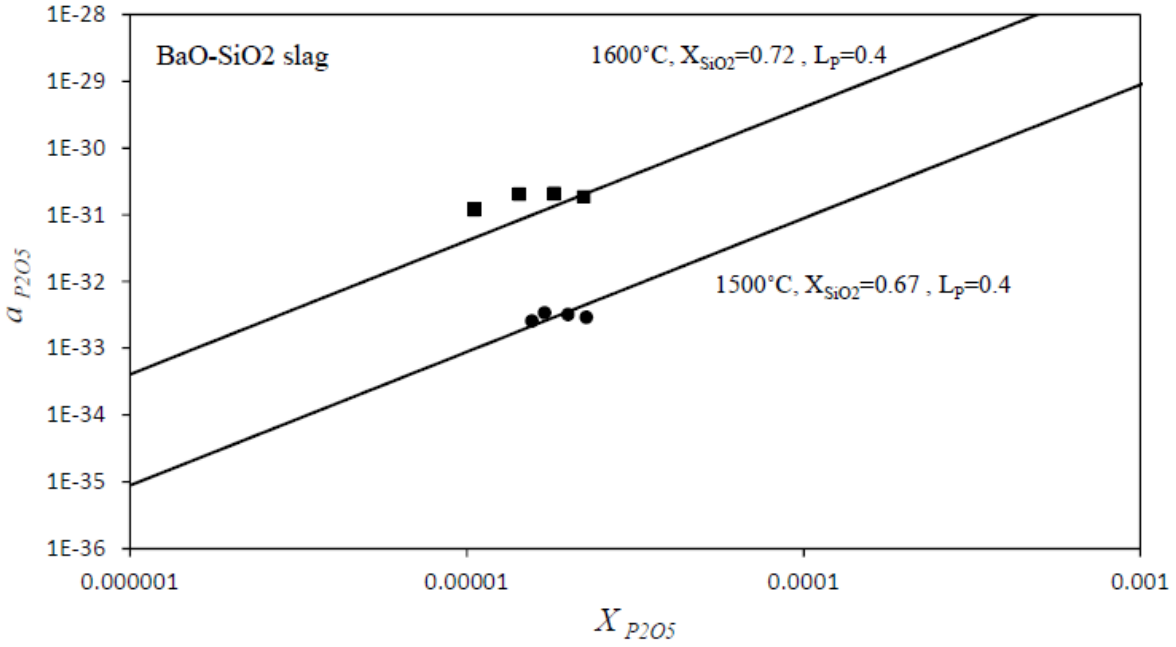
1E-28
1E-29
1E-30
1E-31
1E-32
1E-33
1E-34
1E-35
1E-36
a_{P2O5}
BaO-SiO2 slag
1600°C, X_{SiO2}=0.72 , L_P=0.4
1500°C, X_{SiO2}=0.67 , L_P=0.4
0.000001
0.00001
0.0001
0.001
X_{P2O5}

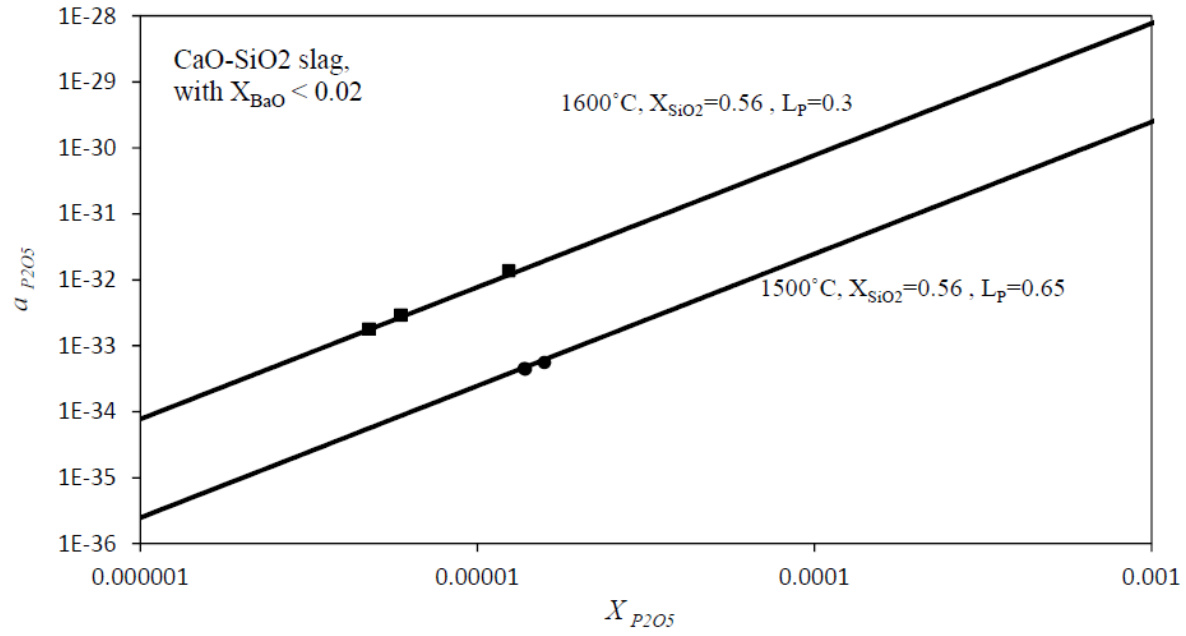
CaO-SiO2 slag,
with $X_{BaO} < 0.02$
1600˚C, X_{SiO2}=0.56 , L_P=0.3
1500˚C, X_{SiO2}=0.56 , L_P=0.65
a_{P2O5}
X_{P2O5}
1E-28
1E-29
1E-30
1E-31
1E-32
1E-33
1E-34
1E-35
1E-36
0.000001
0.00001
0.0001
0.001

Fig. 11

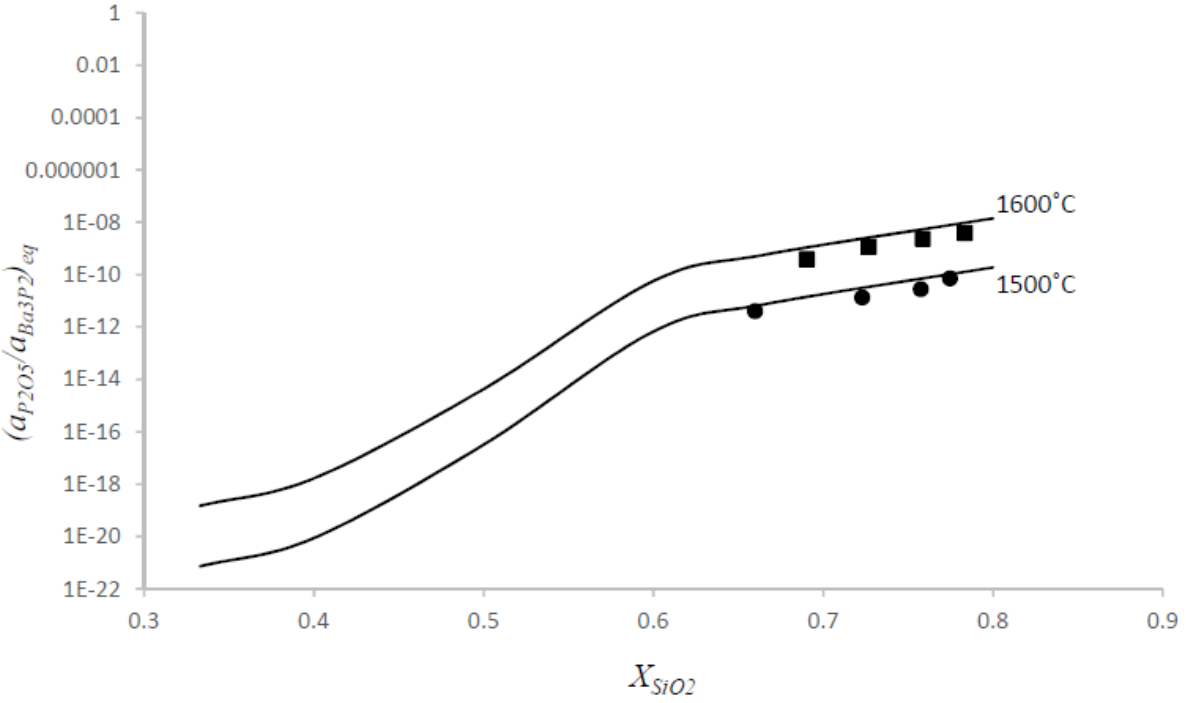
$(a_{P2O5}/a_{Ba3P2})_{eq}$
X_{SiO2}
1600˚C
1500˚C
1
0.01
0.0001
0.000001
1E-08
1E-10
1E-12
1E-14
1E-16
1E-18
1E-20
1E-22
0.3
0.4
0.5
0.6
0.7
0.8
0.9

Fig. 12

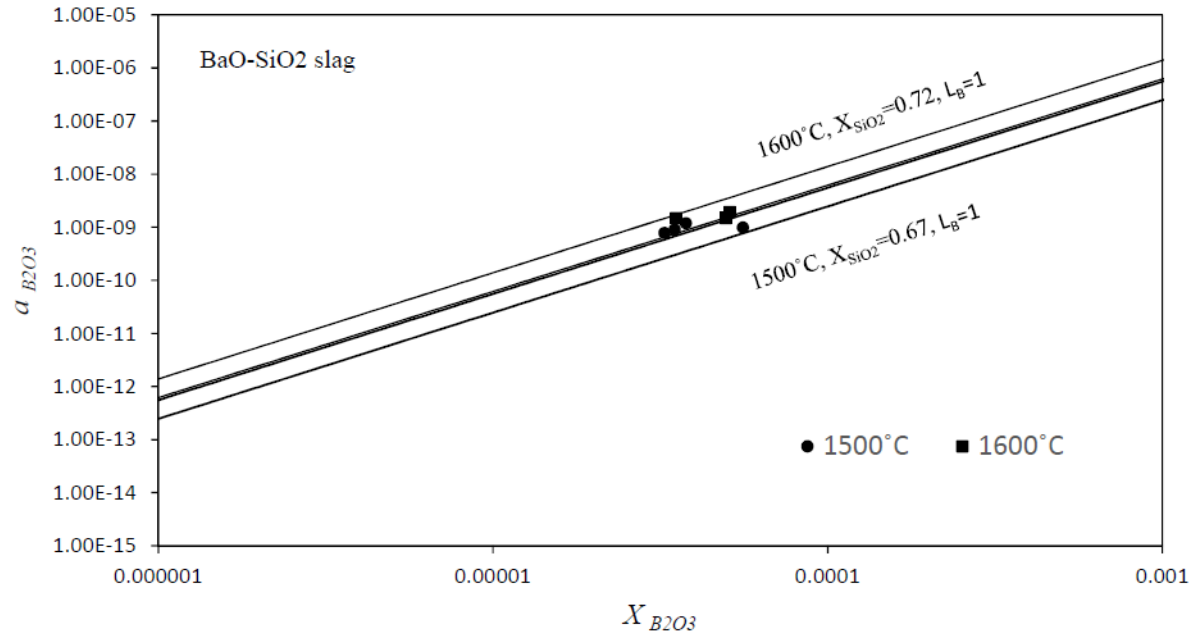
BaO-SiO2 slag
1600˚C, X_{SiO2}=0.72, L_B=1
1500˚C, X_{SiO2}=0.67, L_B=1
● 1500˚C ■ 1600˚C
a_{B2O3}
X_{B2O3}
1.00E-05
1.00E-06
1.00E-07
1.00E-08
1.00E-09
1.00E-10
1.00E-11
1.00E-12
1.00E-13
1.00E-14
1.00E-15
0.000001
0.00001
0.0001
0.001

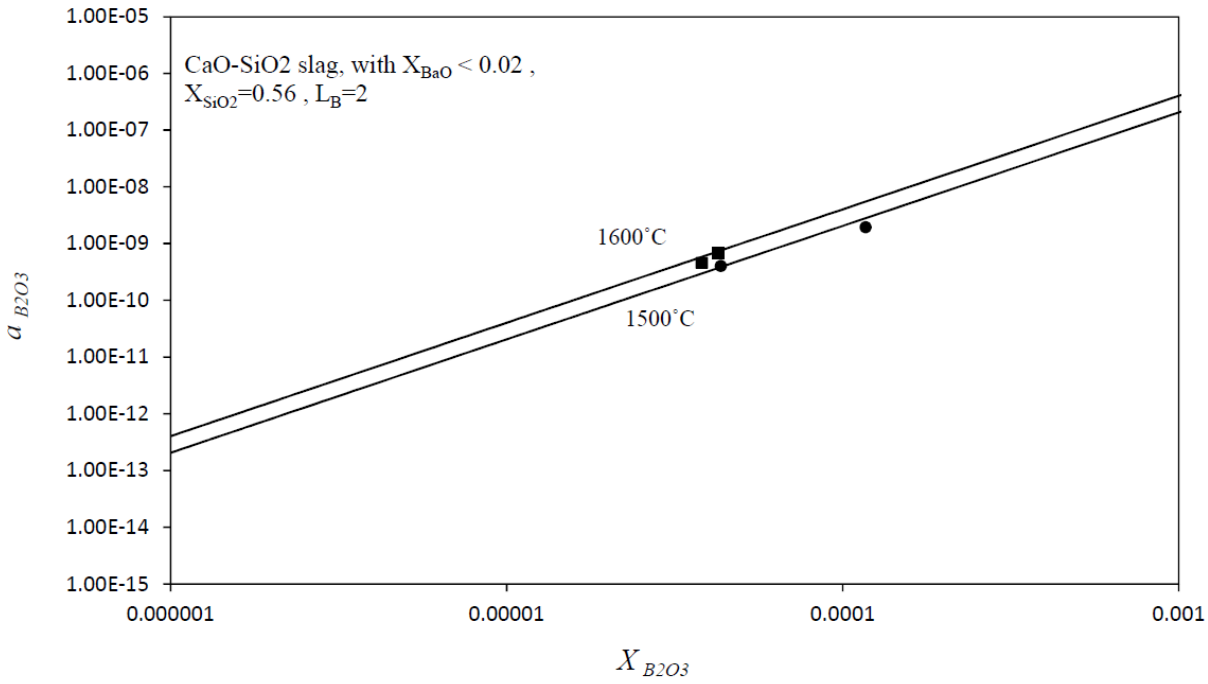
CaO-SiO2 slag, with X_{BaO} < 0.02 ,
X_{SiO2}=0.56 , L_B=2
1600˚C
1500˚C
a_{B2O3}
X_{B2O3}
1.00E-05
1.00E-06
1.00E-07
1.00E-08
1.00E-09
1.00E-10
1.00E-11
1.00E-12
1.00E-13
1.00E-14
1.00E-15
0.000001
0.00001
0.0001
0.001

Fig. 13

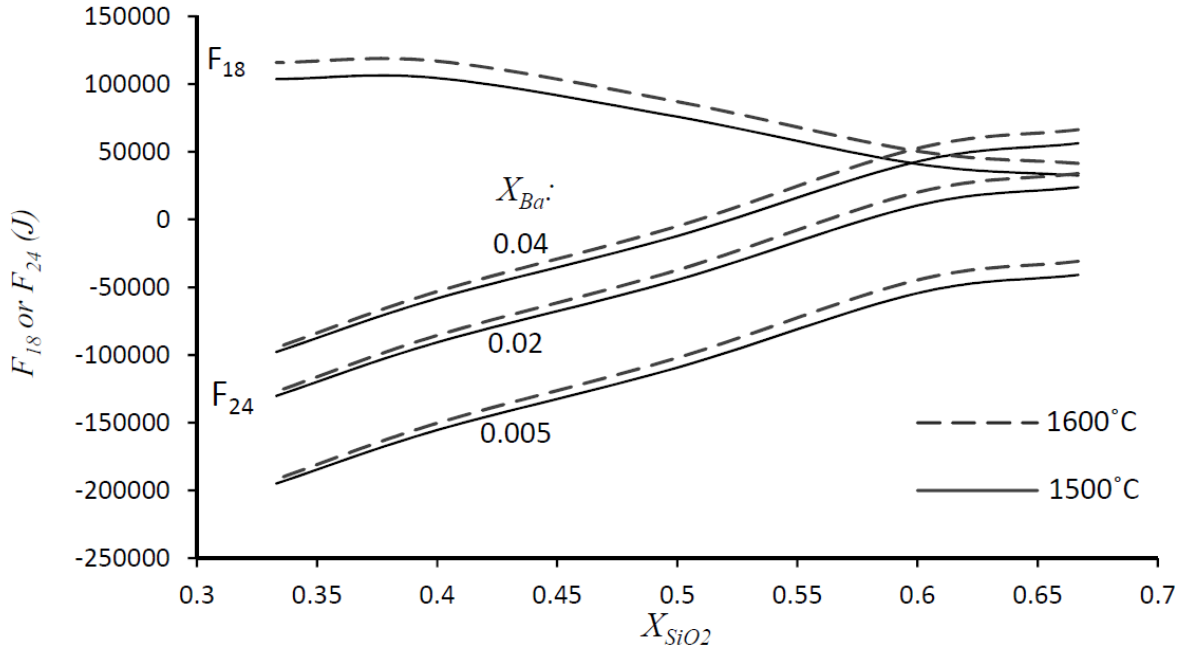
150000
100000
50000
0
-50000
-100000
-150000
-200000
-250000
0.3
0.35
0.4
0.45
0.5
0.55
0.6
0.65
0.7
F18
F24
X_{Ba}:
0.04
0.02
0.005
1600˚C
1500˚C
F_{18} or F_{24} (J)
X_{SiO2}

Fig. 14